

OPTIMIZATION OF THE HGQ IRON YOKE FOR OPERATION AT 4.5 K

V.V. Kashikhin and A.V. Zlobin
Fermilab, P.O. Box 500, Batavia, IL 60510

Abstract - The note reports the results of iron yoke optimization of the high gradient quadrupole developed for the LHC IRs for operation in Tevatron low-beta insertions at 4-4.5 K. The expected magnet performance parameters are also presented.

1. INTRODUCTION

Fermilab in collaboration with LBNL has developed large-aperture high gradient quadrupoles (HGQ) for the LHC inner triplets [1]. These magnets were designed to operate at 1.9 K in superfluid helium providing field gradients up to 215 T/m in the 70 mm bore with large critical current and critical temperature margins required for the operation at high radiation-induced heat depositions in the coil. Magnet design parameters have been optimized and confirmed by a series of short models and the full-scale prototype [2-4]. The production of these magnets for the LHC interaction regions (IR) has been recently started at Fermilab [5].

Large-aperture high-gradient quadrupoles of this type could also be used in other applications, in particular in Tevatron, instead of the obsolete low-beta quadrupoles (LBQ). One of the possible applications could be the new interaction region at C0 being studied for the BTeV experiment. In Tevatron the HGQ magnets will operate at 4.5 K with lower field gradient. The HGQ iron yoke designed for the field gradient up to 250 T/m can be re-optimized resulting in a reduction of the cold mass and cryostat sizes and leading to significant cost saving.

The HGQ iron yoke optimized for operation at 4.5 K is described in this note. During the optimization the collared coil parameters were kept the same preserving all magnet parameters including the field quality and quench performance as they were measured in HGQ short models and prototype. The magnet performance parameters are also reported in the note.

2. IRON YOKE OPTIMIZATION

The cross-section of HGQ is shown in Figure 1. Two-layer collared coil is surrounded by the two-piece iron yoke held together by the welded skin. The iron yoke consists of four large round holes required for the longitudinal heat transfer by superfluid helium from the coil to the external HeII heat exchanger and four large rectangular holes reserved for the high-current bus-bars and electrical instrumentation. These holes along with the high nominal field gradient of 215 T/m resulted in the quite large iron yoke outer diameter of 400 mm.

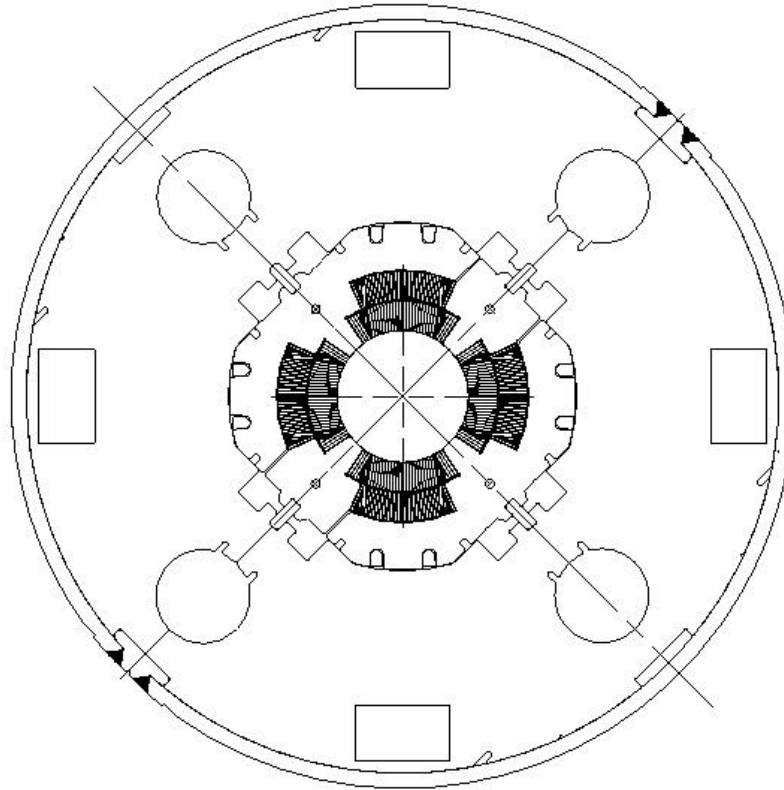


Figure 1. Cross-section of HGQ developed for the LHC IRs.

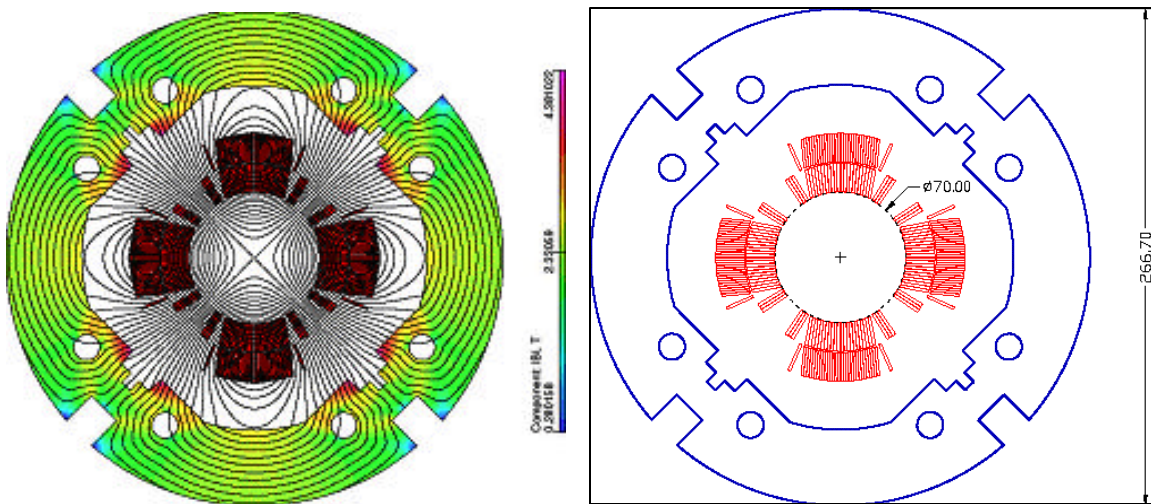


Figure 2. Optimized HGQ magnet cross-section.

The optimization goals were reduction of the iron yoke OD from 400 mm to 267 mm as in LBQ and optimization of the iron yoke cross-section providing the holes for power and instrumentation cables and channels for the liquid helium flow, and minimizing the iron saturation effect. The inner shape and the size of the new iron yoke is similar to the shape of the HGQ collared coil. The collared coil is supported and aligned inside the

yoke with a help of special alignment keys. As in HGQ there is a small gap between the collar and yoke excluding the yoke from the coil mechanical support structure.

The field quality was optimized using OPERA2D code. In order to reduce the iron saturation effect to the tolerable limits, eight round holes were used. The position and size of the holes were optimized to restrict the field quality deviations due to the yoke saturation effect within $0.15 \cdot 10^{-4}$.

Figure 1 shows the optimized iron yoke geometry and the flux distribution in the magnet cross-section. Two $18.5 \times 18.5 \text{ mm}^2$ rectangular holes are sufficient to accommodate 4-6 pairs of 12-15 kA stabilized electrical bus-bars described in [6] and the other two rectangular holes could house the necessary instrumentation wires and cables. If required the size of these holes could be increased without dramatical effect on the magnet field quality. Eight round holes with total cross-section area of 14 cm^2 and 1-2 mm annular channel provide sufficient cross-section for the helium flow inside the magnet cold mass.

3. MAGNET PERFORMANCE

In this section the magnet performance parameters at 4.5 K are reported based on the results obtained on last HGQ short models and full-scale prototype. This approach is valid since the iron yoke is not an element of coil support structure before and after optimization.

3.1. Magnet training

The training at 4.5 K of optimized magnets could be estimated based on the training of few last short models HGQ05-07 with optimized mechanical design and trained at 4.5 K. The results are shown in Figure 3. The variations of the maximum current reached during training are due to the variations of critical current density of NbTi strands used in those models.

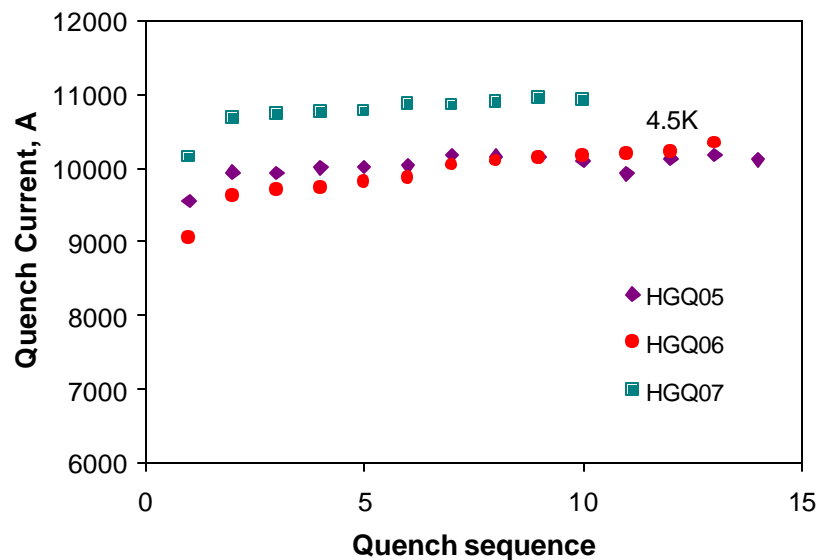


Figure.3. Magnet training (HGQ05-07) at 4.5 K.

3.2. Temperature dependence of magnet short sample limit

The dependence of magnet quench current vs. the temperature for HGQ05-09 is presented in Figure 4. Solid line shows the generic short sample limit for this magnet design calculated based on the SSC strand specifications. The data show that this type of magnets can reach its short sample limit at temperature above 3.5 K and operate at currents up to 10 kA at temperatures 4.5 K.

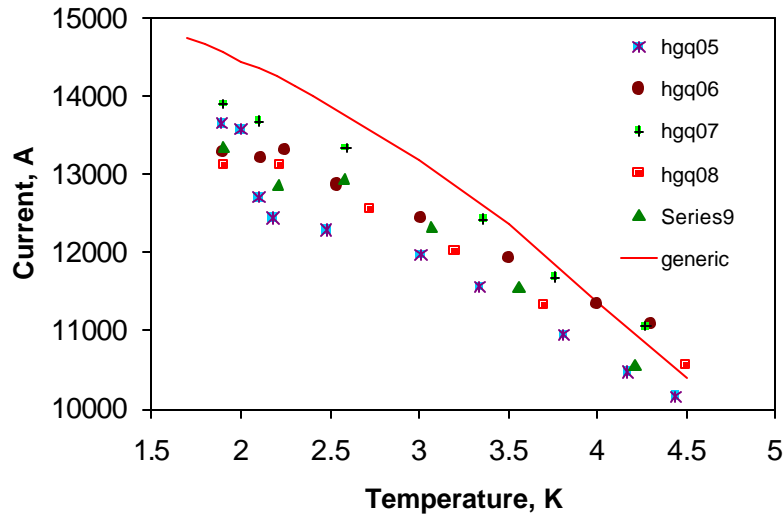


Figure 4. Temperature dependence of HGQ05-09 quench current.

3.3. Ramp rate sensitivity of magnet quench current

The typical dependence of magnet quench current at 1.9 K vs. the current ramp rate for HGQ05 and HGQ09 fabricated using the optimized coil curing cycle, is shown in Figure 5. Similar performance is expected for this type of magnets at higher temperatures.

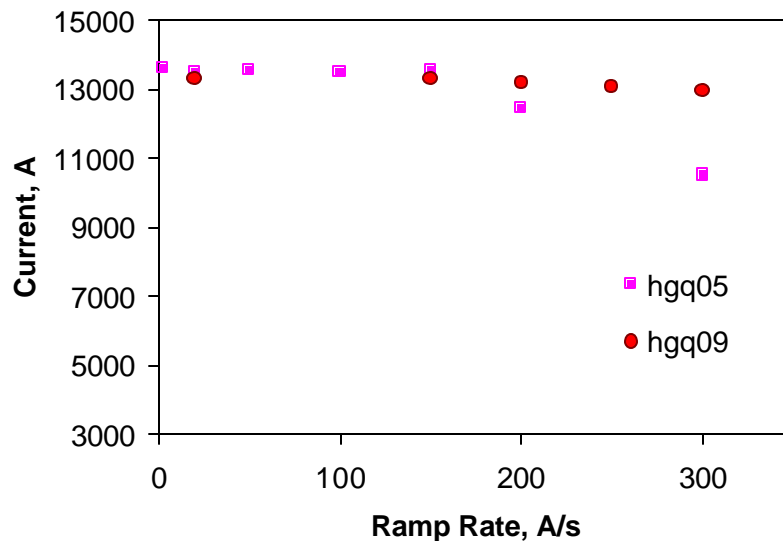


Figure 5. HGQ05 and HGQ09 quench current ramp rate dependence at 1.9 K.

3.4. AC losses

The expected level of AC losses in HGQ magnets with optimized coil curing cycle, represented by HGQ03A and HGQ05, is shown in Figure 6.

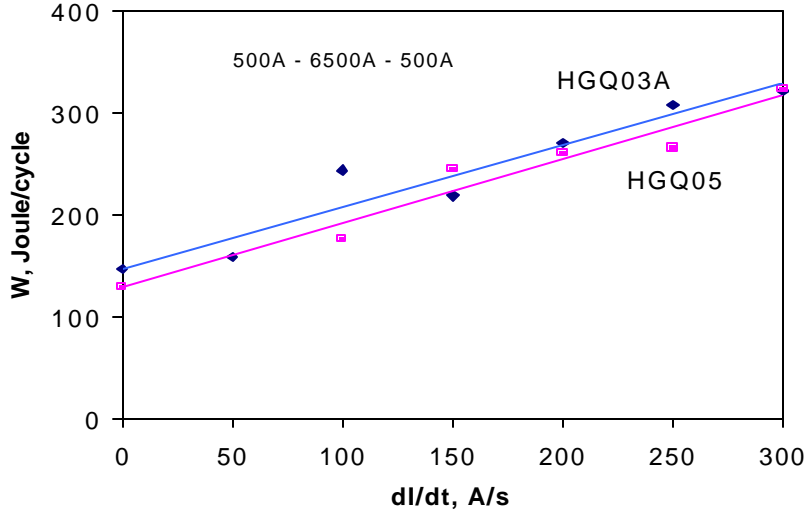


Figure 6. AC losses in the triangular cycle with current amplitude change within 500-6500 A range vs. the current ramp rate.

3.5. Magnet transfer function

Figure 7 shows the measured and calculated transfer function for the HGQ short models as a function of current. As it can be seen, there is a good correlation between measured and calculated data at all currents in the magnet. The reduction of the magnet transfer function at high currents is caused by the iron saturation. At operation current of 10 kA the nominal field gradient is 180 T/m.

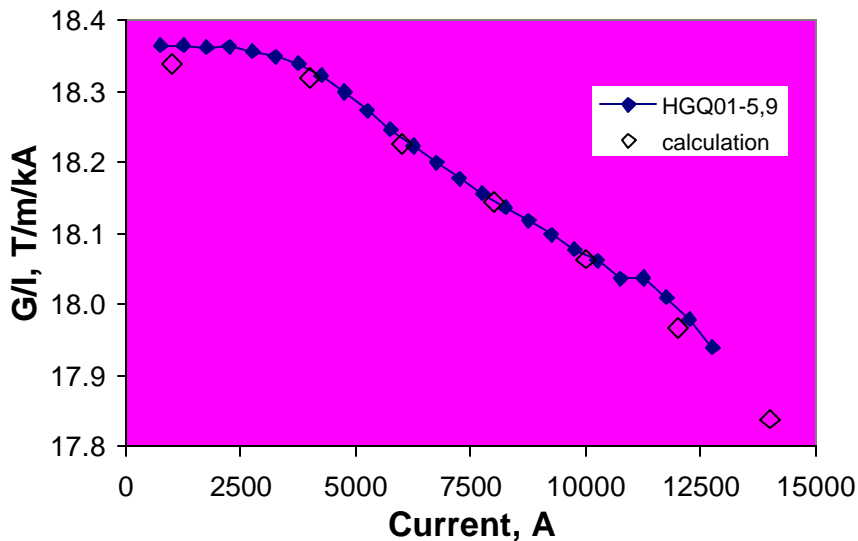


Figure 7. Measured and calculated magnet transfer function.

3.6. Body field harmonics

In the magnet body the field is represented in terms of harmonic coefficients defined by the power series expansion

$$B_y(x, y) + iB_x(x, y) = 10^{24} B_2 \sum_{n=1}^{\infty} (b_n + ia_n) \left(\frac{x + iy}{R_{ref}} \right)^{n+1},$$

where $B_x(x, y)$ and $B_y(x, y)$ are the transverse field components, B_2 is the quadrupole field strength, b_n and a_n are the “normal” and “skew” harmonic coefficients ($b_2=10^4$) at a reference radius R_{ref} of 17 mm.

The coordinate system for magnetic measurement is defined with the z -axis at the center of the magnet aperture and pointing from return to lead end with the origin at the boundary between return end and straight section. The x -axis is horizontal and pointing right, and the y -axis, vertical and pointing up to the observer who faces the magnet lead end.

Table 1 shows mean values and RMS spread at $R_{ref}=17$ mm of low-order field harmonics over the last five short models HGQ05-09 measured at 6 kA current.

Table 1. Averages and Standard Deviations of field harmonics for HGQ05-09.

	Mean	RMS
b_3	0.49	0.26
a_3	0.12	0.28
b_4	-0.01	0.08
a_4	-0.15	0.37
b_5	-0.02	0.07
a_5	-0.06	0.15
b_6	-0.23	0.17
a_6	-0.03	0.05
b_7	0.01	0.03
a_7	0.02	0.03
b_8	0.00	0.01
a_8	0.00	0.01
b_9	0.00	0.00
a_9	0.00	0.01
b_{10}	0.00	0.01
a_{10}	0.00	0.00

The expected shift of b_6 from the value presented in the Table 1 at 800 A current due to the coil magnetization effect is $-(1.2-1.3)$ units at 4.5 K. Its decay during first 900 s is less than 0.4 units. The effect of iron saturation on b_6 and b_{10} in HGQ with the optimized iron yoke is show in Figure 8.

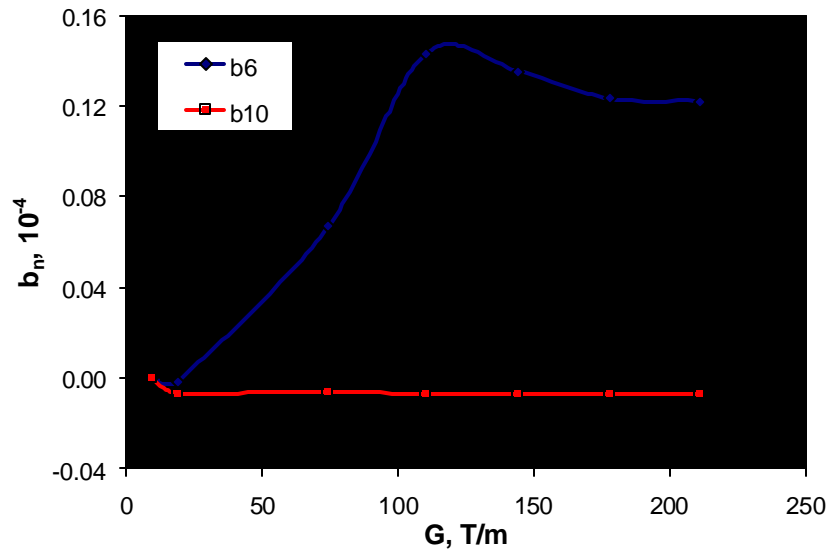


Figure 8. The yoke saturation effect.

4. CONCLUSIONS

Optimized HGQ magnets described in this note provide the nominal field gradients up to 180 T/m at operation temperatures 4.5 K or less, with nominal current up to 10 kA and current ramp rates less than 150-200 A/s and excellent reproducible field quality.

REFERENCES

- [1] R. Bossert et al., “Development of a High Gradient Quadrupole for the LHC Interaction Regions”, IEEE Trans. on Applied Superconductivity, Vol. 7, No 2, June 1997, p. 751.
- [2] N. Andreev et al., “Quench and Mechanical Performance for Fermilab Model Magnets for the LHC Inner Triplet Quadrupoles”, Presented at ASC 2000, Virginia Beach, VA.
- [3] N. Andreev et al., “Field Quality in Fermilab-Built Models of Quadrupole Magnets for the LHC Interaction Region”, Presented at ASC 2000, Virginia Beach, VA.
- [4] R. Bossert et al., “Quench Performance and Mechanical Behavior of the First Fermilab-built Prototype High Gradient Quadrupole for the LHC Interaction Regions”, Presented at MT-17, Geneva, Switzerland.
- [5] R. Bossert et al., “Production and Test of the First LQXB Inner Triplet Quadrupole at Fermilab”, Presented at EPAC 2002, Paris, France.
- [6] P. Bauer et al., “Busbar Studies for the LHC Interaction Region Quadrupoles” Presented at ASC 2000, Virginia Beach, VA.